An Analytical Approach to Asymmetrical Cold Strip Rolling Using the Slab Method

Y.-M. Hwang and G.-Y. Tzou

An analytical model for general asymmetrical cold rolling is proposed to investigate the behavior of sheet during asymmetrical rolling using the slab analysis. Neutral points between the upper and lower rolls and the strip, rolling pressure distribution along the contact interface of the roll and strip, and rolling forces, as well as rolling torque, can be calculated easily using this model. Rolling pressure distribution, rolling force, and rolling torque, which are affected by various rolling conditions such as roll speed ratio, thickness reduction, front and back tension, etc., are analyzed. Additionally, the limiting rolling conditions between reduction and roll speed ratio, or front and back tension, under which the rolling process can be accomplished successfully, are discussed. By comparing analytical results and experimental measurements of rolling force, it is apparent that the proposed model can successfully provide useful knowledge for designing the pass schedule of the asymmetrical cold strip rolling process.

Keywords
cold rolling, slab method, strip rolling

1. Introduction

ANALYSIS of symmetrical strip rolling, in which the peripheral velocity and radius of the upper roll are equal to those of lower roll, respectively, has been discussed[1-3] in detail since Orowan[4] proposed a uniform plastic deformation model of strip rolling. The plastic deformation mechanism of strip during symmetric strip rolling at the roll-bite has been clarified. Recently, the asymmetrical strip rolling process, in which the peripheral velocity and radius of the upper roll are different from those of the lower roll, has been studied. This process has become increasingly important, because it offers benefits such as less rolling pressure, less rolling force, less rolling torque, and improved strip surface properties compared to those obtained by symmetric strip rolling. Most investigations concerning asymmetrical cold strip rolling are experimental,[5-12] a few numerical analyses were carried out using the slab method and the finite-element method.[13-15] However, significant calculation time and computer expense are required, and use of this analysis in asymmetric cold strip rolling has not been well established.

In this study, an analytical solution for asymmetrical strip rolling is proposed using the slab method. Using this approach, rolling pressure distribution, rolling force, and rolling torque can be easily and rapidly obtained. Effects of rolling speed ratio, rolling radius ratio, frictional coefficient ratio, etc., on rolling pressure distribution, rolling force, and rolling torque are discussed systematically.

Y.-M. Hwang and **G.-Y. Tzou,** Department of Mechanical Engineering, National Sun Yat-Sen University, Kaohsiung, Taiwan 80424, Republic of China.

2. Mathematical Model

To simplify the formulation involved in developing the analysis in cold rolling based on the slab method, the following assumptions were made:

- The roll is rigid; the strip being rolled is rigid-plastic material.
- Plastic deformation is plane-strain.
- Stresses are uniformly distributed within elements. The vertical stress (p) and horizontal stress (q) are regarded as principal stresses.
- Frictional coefficients between the roll and material are constant over the arc of contact, but the coefficient for the upper roll may be different from that of the lower roll.
- The flow direction of the strip at the entrance and exit of the roll-bite is horizontal

Nomenclature

L = Length of contact
P = Rolling force per width
T = Total calculated rolling torque per width
p = Vertical stress
q = Horizontal stress
x = Horizontal distance from exit point of roll-bite
h = Variable strip thickness
k = Material yield strength in shear
r = Reduction
q_i = Back tension
q_o = Front tension
h_o = Final strip thickness
h_i = Initial strip thickness
R_1, R_2 = Radius of upper roll and lower roll, respectively
T_1, T_2 = Rolling torque of upper roll and lower roll, respectively
σ_{yp} = Uniaxial yield stress
μ_1, μ_2 = Coefficients of friction of upper roll and lower roll, respectively
θ_1, θ_2 = Variable angles of contact of upper roll and lower roll, respectively
V_1, V_2 = Peripheral speeds of upper roll and lower roll, respectively
p_1, p_2 = Specific rolling pressures of upper roll and lower roll, respectively

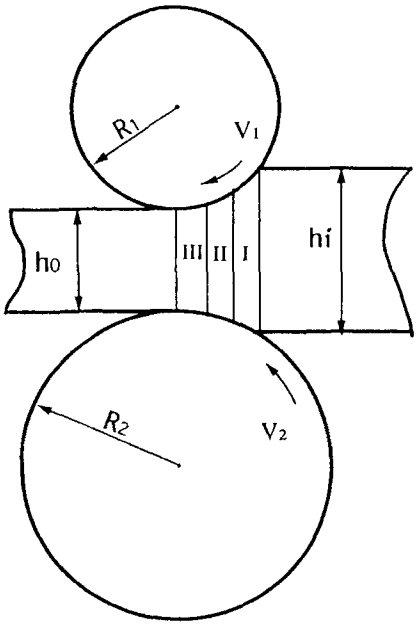

Fig. 1 Schematic of mathematical model.

- The total roll contact arc is small compared to the circumference of the roll.

These assumptions provide a physically realistic approximation of the cold rolling processes of thin wide strip or sheet.

2.1 *Formulation*

Figure 1 is a schematic illustration of asymmetric strip rolling. The radius and speed of the upper roll are different from those of the lower roll. The plastic deformation region at the roll-bite is divided into three distinct regions according to the directions of frictional force from the upper and lower roll exerted on the strip. These are denoted zone I for entry regions, zone II for the cross shear region, and zone III for the exit region, as shown in Fig. 1. The subscripts 1 and 2 in all variables denote the upper and lower rolls, respectively.

Figure 2 illustrates the stress state of a slab in zone I, in which the directions of the upper and lower frictional forces are both forward, i.e., the velocities of the upper and lower rolls are both faster than that of the strip. Because the position of the neutral point on the upper roll is not necessarily equal to that of the lower roll, the direction of the frictional force from the upper roll exerted on the strip may not be the same as that from the lower roll.

The mathematical expressions for the horizontal and vertical force equilibria are summarized as:

$$\frac{d(hq)}{dx} + p_1 \tan\theta_1 + p_2 \tan\theta_2 - (\tau_1 + \tau_2) = 0 \qquad [1]$$

$$p = p_1(1 + \mu_1 \tan\theta_1) = p_2(1 + \mu_2 \tan\theta_2) \qquad [2]$$

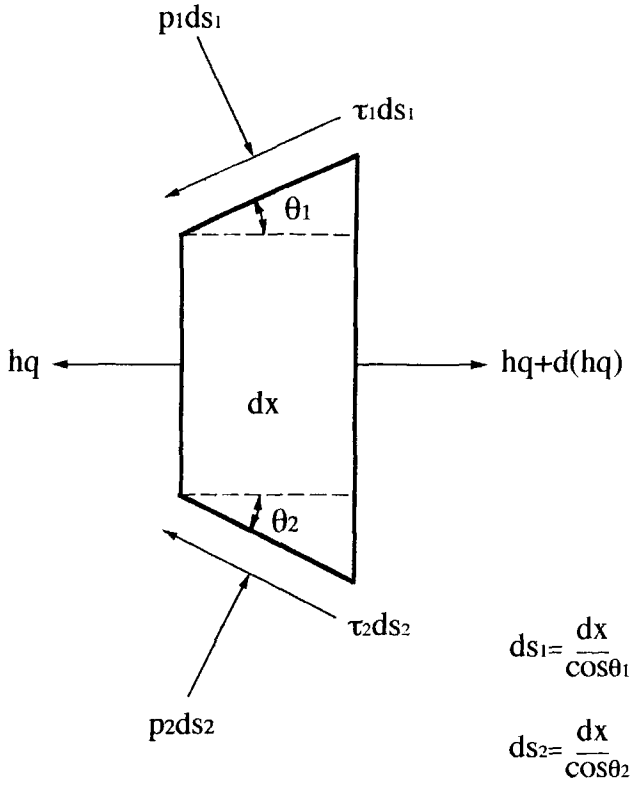

Fig. 2 Material elements in region I.

where q is the horizontal stress; h is the thickness; and p_1 and p_2 are the normal pressure from the upper and lower roll, respectively. θ_1 and θ_2 are variable contact angles; $\tau_1 = \mu_1 p_1$ and $\tau_2 = \mu_2 p_2$ are the frictional stresses along the upper and lower roll boundaries, respectively.

Because the roll radius is much larger than the strip thickness, $1 + \mu_1 \tan\theta_1$ and $1 + \mu_2 \tan\theta_2$ in Eq 2 are approximately equal to 1, indicating that $p = p_1 = p_2$.

Combining Eq 1 and 2 gives:

$$h\frac{dq}{dx} + (p + q)\frac{dh}{dx} = \mu_e p \qquad [3]$$

where

$$\mu_e = \mu_1 + \mu_2$$

μ_e is the equivalent frictional coefficient.

The von Mise's yielding criterion for plane-strain can be expressed as

$$p + q = 2k \qquad [4]$$

where k is the yielding shear stress of the material.

Substituting Eq 4 into Eq 3 and rearranging it, yields:

$$(1 + z^2)\frac{df}{dz} + af = 2z \qquad [5]$$

where

$$a = \mu_e\sqrt{P\frac{R_{eq}}{h_o}}, R_{eq} = \frac{2R_1R_2}{R_1 + R_2}$$

$$z = \frac{x}{\sqrt{R_{eq}h_o}}, f = \frac{p}{2k}$$

h_o is the final strip thickness, and R_{eq} is the effective roll radius. Introducing parameter ω as

$$z = \tan\omega \qquad [6]$$

Equation 5 becomes

$$\frac{df}{d\omega} + af = 2\tan\omega \qquad [7]$$

Traditionally, when θ is small, $\tan\omega$ in Eq 7 can be approximately expressed as

$$\tan\omega \fallingdotseq \omega \qquad [8]$$

However, more precisely, one adopts

$$\tan\omega \fallingdotseq \omega + \frac{\omega^3}{3} \qquad [9]$$

The solution of the differential Eq 7 is

$$f = ce^{-a\omega} + \frac{2}{a}\left[\frac{\omega^3}{3} - \frac{\omega^2}{a} + s\omega - t\right] \qquad [10]$$

where

$$s = 1 + \frac{2}{a^2}, t = \frac{1}{a} + \frac{2}{a^3}$$

where c is the integral constant determined by the boundary condition.

In zone III, because the direction of the friction forces is backward, i.e., the strip velocity is faster than the velocity of the upper and lower roll, the form of the differential equation in zone III is the same as that in zone I. Only the effective coefficient of friction μ_e is replaced by $\mu_e = -\mu_1 - \mu_2$.

In zone II, because the directions of the frictional forces cross each other, i.e., the strip velocity is faster than the velocity of the upper roll and slower than the velocity of the lower roll (in the case of $V_2 > V_1$), $\mu_e = -\mu_1 + \mu_2$.

2.2 *Boundary Conditions*

Assuming that the velocity of the lower roll is faster than that of the upper roll, the neutral point of the upper roll is denoted by x_{n1}, and the neutral point of the lower roll is denoted x_{n2}. Thus, the boundary conditions for three distinct regions can be expressed as follows:

2.2.1 Zone III ($0 \le x \le x_{n2}$) $\mu_e = -\mu_1 - \mu_2$

At $x = 0$ (or $\omega = 0$)

$$f_0 = 1 - \frac{q_o}{2k}$$

where q_o is the front tension exerted on the strip.

From this boundary condition, the integral constant c_3 in Eq 10 can be obtained as

$$c_3 = f_o + \frac{2t_3}{a_3} \qquad [11]$$

where

$$t_3 = \frac{1}{a_3} + \frac{2}{a_3^3}, s_3 = 1 + \frac{2}{a_3^2}$$

Hence, the specific rolling pressure (f_{III}) in zone III is expressed as

$$f_{III} = \left(f_o + \frac{2t_3}{a_3}\right)e^{-a_3\omega} + \frac{2}{a_3}\left[\frac{\omega^3}{3} - \frac{\omega^2}{a_3} + s_3\omega - t_3\right] \qquad [12]$$

2.2.2 Zone I ($x_{n1} \le x \le L$) $\mu_e = \mu_1 + \mu_2$

At $x = L$ (or $\omega = \omega_i = \tan^{-1}L/\sqrt{R_{eq}h_o}$)

$$f_i = 1 - \frac{q_i}{2k}$$

where q_i is the back tension exerted on the strip.

From this boundary condition, c_1 is expressed as

$$c_1 = B_i e^{a_1\omega_i} \qquad [13]$$

Therefore, the specific rolling pressure (f_1) in zone I is expressed as

$$f_1 = B_i e^{a_1\omega_i} e^{-a_1\omega} + \frac{2}{a_1}\left[\frac{\omega^3}{3} - \frac{\omega^2}{a_1} + s_1\omega - t_1\right] \qquad [14]$$

where

$$t_1 = \frac{1}{a_1} + \frac{2}{a_1^3}$$

$$B_i = f_i - \frac{2}{a_1}\left[\frac{\omega_i^3}{3} - \frac{\omega_i^2}{a_1} + s_1\omega_i - t_1\right]$$

$$s_1 = 1 + \frac{2}{a_1^2}$$

When the peripheral velocity of the upper roll (V_1) is less than that of the lower roll (V_2), zone II is $x_{n2} \le x \le x_{n1}$ and $\mu_e = -\mu_1 + \mu_2$.

2.2.3 Zone II ($x_{n2} \le x \le x_{n1}$) $\mu_e = -\mu_1 + \mu_2$

Due to the continuity of the boundary conditions at $x = x_{n2}$ (or $\omega = \omega_{n2}$), the specific rolling pressure in zone III (f_{III}) at $x = x_{n2}$ must be equal to that in zone II (f_{II}), i.e., $f_{III} = f_{II}$. Therefore, c_3 and c_2 have a relationship as follows:

$$c_3 e^{-a_3\omega_{n2}} + \frac{2}{a_3}\left[\omega_{n2}^3 - \frac{\omega_{n2}^2}{a_3} + s_3\omega_{n2} - t_3\right]$$

$$c_2 e^{-a_2\omega_{n2}} + \frac{2}{a_2}\left[\frac{\omega_{n2}^3}{3} - \frac{\omega_{n2}^2}{a_2} + s_2\omega_{n2} - t_2\right] \qquad [15]$$

However, due to the continuity of the boundary conditions at $x = x_{n1}$, i.e., $f_I = f_{II}$

$$c_1 e^{-a_1\omega_{n1}} + \frac{2}{a_1}\left[\omega_{n1}^3 - \frac{\omega_{n1}^2}{a_1} + s_1\omega_{n1} - t_1\right] = c_2 e^{-a_2\omega_{n1}} + \frac{2}{a_2}\left[\frac{\omega_{n1}^3}{3} - \frac{\omega_{n1}^2}{a_2} + s_2\omega_{n1} - t_2\right] \qquad [16]$$

From Eq 15, c_2 is expressed as

$$c_2 = c_3 e^{B_1\omega_{n2}} + e^{a_2\omega_{n2}}\left(B_2\omega_{n2}^3 - B_3\omega_{n2}^2 + B_4\omega_{n2} - B_5\right) \qquad [17]$$

where

$$B_1 = a_2 - a_3,\ B_2 = \frac{2}{3a_3} - \frac{2}{3a_2}$$

$$B_3 = \frac{2}{a_3^2} - \frac{2}{a_2^2},\ B_4 = \frac{2S_3}{a_3} - \frac{2S_2}{a_2}$$

$$B_5 = \frac{2t_3}{a_3} - \frac{2t_2}{a_2}$$

Substituting Eq 17 into Eq 16 yields

$$c_1 e^{B_6\omega_{n1}} + \frac{2e^{a_2\omega_{n1}}}{a_1}\left[\frac{\omega_{n1}^3}{3} - \frac{\omega_{n1}^2}{a_1} + s_1\omega_{n1} - t_1\right] - \frac{2}{a_2}e^{a_2\omega_{n1}}\left(\frac{\omega_{n1}^3}{3} - \frac{\omega_{n1}^2}{a_2} + s_2\omega_n\right) - c_3 e^{B_1\omega_{n2}} - e^{a_2\omega_{n2}}\left(B_2\omega_{n2}^3 - B_3\omega_{n2}^2 + B_4\omega_{n2} - B_5\right) = 0 \qquad [18]$$

where

$$\omega_{n1} = \tan^{-1}\frac{x_{n1}}{\sqrt{R_{eq}h_o}},\ \omega_{n2} = \tan^{-1}\frac{x_{n2}}{\sqrt{R_{eq}h_o}}$$

$$B_6 = a_2 - a_1$$

From the constancy of volume, the positions of the upper and lower neutral points x_{n1} and x_{n2} have the following relationship:

$$x_{n1} = R_1\sqrt{V_A\frac{x_{n2}^2}{R_1^2} + (V_A - 1)\frac{h_o}{R_A}} \qquad [19]$$

where

$$V_A = \frac{V_2}{V_1},\ R_A = \frac{R_1}{2}\left(1 + \frac{R_1}{R_2}\right)$$

Substitute Eq 19 into Eq 18, the solution of the neutral point x_{n2} can be determined easily using the bisection numerical method. Because x_{n2} is known, x_{n1} and c_2 can be obtained by Eq 17 and 19.

Then, the specific rolling pressure (f_{II}) in zone II can be obtained as:

$$f_{II} = c_2 e^{-a_2\omega} + \frac{2}{a_2}\left[\frac{\omega^3}{3} - \frac{\omega^2}{a_2} + s_2\omega - t_2\right] \qquad [20]$$

where

$$t_2 = \frac{1}{a_2} + \frac{2}{a_2^3},\ s_2 = 1 + \frac{2}{a_2^2}$$

2.3 *Rolling Force*

Once the yielding stress and coefficient of friction are known, the rolling force can be found by integrating the normal rolling pressure over the arc length of contact. Thus, the rolling force per unit width is given by:

$$P = P_{III} + P_{II} + P_I \qquad [21]$$

where

$$P_{III} = 2k\int_0^{x_{n2}} f_{III}dx = 2k\sqrt{R_{eq}h_o}(III_1 + III_2) \quad [22]$$

$$III_1 = \frac{-c_3 e^{-a_3\omega_{n2}}}{a_3}\left(1 + \omega_{n2}^2 + \frac{2\omega_{n2}}{a_3} + \frac{2}{a_3^2}\right) + \frac{c_3}{a_3} + \frac{2c_3}{a_3^3}$$

$$III_2 = \frac{\omega_{n2}^6}{9a_3} - \frac{2\omega_{n2}^5}{5a_3^2} + \frac{1/3 + s_3}{2a_3}\omega_{n2}^4 - \frac{2}{3a_3}\left(\frac{1}{a_3} + t_3\right)\omega_{n2}^3 + \frac{s_3\omega_{n2}^2}{a_3} - \frac{2t_3\omega_{n2}}{a_3}$$

$$P_{II} = 2k\int_{x_{n2}}^{x_{n1}} f_{II}dx = 2k\sqrt{R_{eq}(h_o}(II_1 + II_2) \quad [23]$$

$$II_1 = \frac{-c_2 e^{-a_2\omega_{n1}}}{a_2}\left(1 + \omega_{n1}^2 + \frac{2\omega_{n1}}{a_2} + \frac{2}{a_2^2}\right) + \frac{\omega_{n1}^6}{9a_2} - \frac{2\omega_{n1}^5}{5a_2^2} + \frac{1/3 + s_2}{2a_2}\omega_{n1}^4 - \frac{2}{3a_2}\left(\frac{1}{a_2} + t_2\right)\omega_{n1}^3 + \frac{s_2}{a_2}\omega_{n1}^2 - \frac{2t_2}{a_2}\omega_{n1}$$

$$II_2 = \frac{c_2 e^{-a_2\omega_{n2}}}{a_2}\left(1 + \omega_{n2}^2 + \frac{2\omega_{n2}}{a_2} + \frac{2}{a_2^2}\right) - \frac{\omega_{n2}^6}{9a_2} + \frac{2\omega_{n2}^5}{5a_2^2} - \frac{1/3 + s_2}{2a_2}\omega_{n2}^4 + \frac{2}{3a_2}\left(\frac{1}{a_2} + t_2\right)\omega_{n2}^3 - \frac{s_2}{a_2}\omega_{n2}^2 + \frac{2t_2}{a_2}\omega_{n2}$$

$$P_I = 2k\int_{x_{n1}}^{L} f_I dx = 2k\sqrt{R_{eq}h_o}(I_1 + I_2) \quad [24]$$

$$I_1 = \frac{-c_1 e^{-a_1\omega_i}}{a_1}\left(1 + \omega_i^2 + \frac{2\omega_i}{a_1} + \frac{2}{a_1^2}\right) + \frac{\omega_i^6}{9a_1} - \frac{2\omega_i^5}{5a_1^2} + \frac{1/3 + s_1}{2a_1}\omega_i^4 - \frac{2}{3a_1}\left(\frac{1}{a_1} + t_1\right)\omega_i^3 + \frac{s_1\omega_i^2}{a_1} - \frac{2t_1\omega_i}{a_1}$$

$$I_2 = \frac{c_1 e^{-a_1\omega_{n1}}}{a_1}\left(1 + \omega_{n1}^2 + \frac{2\omega_{n1}}{a_1} + \frac{2}{a_1^2}\right) - \frac{\omega_{n1}^6}{9a_1} + \frac{2\omega_{n1}^5}{5a_1^2} - \frac{1/3 + s_1}{2a_1}\omega_{n1}^4 + \frac{2}{3a_1}\left(\frac{1}{a_1} + t_1\right)\omega_{n1}^3 - \frac{s_1\omega_{n1}^2}{a_1} + \frac{2t_1\omega_{n1}}{a_1}$$

2.4 *Rolling Torque*

The rolling torque, T_1 and T_2, exerted by strip on the upper and lower roll, respectively, can be calculated by integrating the moment of the frictional force along the arc of contact about the roll axis. Therefore:

$$T_1 = R_1(\mu_1 P_I - \mu_1 P_{II} - \mu_1 P_{III}) = \mu_1 R_1(P_I - P_{II} - P_{III}) \quad [25]$$

$$T_2 = R_2(\mu_2 P_I + \mu_2 P_{II} - \mu_2 P_{III}) = \mu_2 R_2(P_I + P_{II} - P_{III}) \quad [26]$$

2.5 *Special Case*

When the frictional coefficient between the upper roll and the strip (μ_1) is equal to the frictional coefficient between the lower roll and strip (μ_2), Eq 11 and 12 are still valid. However, both Eq 20 and 23 no longer apply, because μ_e (or a_2) is zero in zone II. Therefore, the equations derived previously concerning pressure distribution become meaningless and modifications have to be made.

From Eq 3, let μ_e be zero, the specific rolling pressure in zone II can be expressed as:

$$f_{II} = \ln h + c_2 \quad [27]$$

where c_2 is the integral constant determined by the boundary conditions.

Following the same procedures with the same boundary conditions as described earlier, the equation that was used to find the neutral point x_{n2} is expressed as:

$$c_1 e^{-a_1\omega_{n1}} + \frac{2}{a_1}\left[\frac{\omega_{n1}^3}{3} - \frac{\omega_{n1}^2}{a_1} + s_1\omega_{n1}\right] - c_3 e^{-a_3\omega_{n2}} - \frac{2}{a_3}\left[\frac{\omega_{n2}^3}{3} - \frac{\omega_{n2}^2}{a_3} + s_3\omega_{n2}\right] - F = 0 \quad [28]$$

where

$$F = \ln\frac{V_2}{V_1} + \frac{2t_1}{a_1} - \frac{2t_3}{a_3}$$

$$\omega_{n1} = \tan^{-1}\frac{x_{n1}}{\sqrt{R_{eq}h_o}}$$

$$\omega_{n2} = \tan^{-1}\frac{x_{n2}}{\sqrt{R_{eq}h_o}}$$

Combining Eq 19 and 28, the neutral point x_{n2} and x_{n1} can be obtained, and c_2 is expressed as:

$$c_2 = c_3 e^{-a_3\omega_{n2}} + \frac{2}{a_3}\left[\frac{\omega_{n2}^3}{3} - \frac{\omega_{n2}^2}{a_3} + s_3\omega_{n2} - t_3\right] - \ln h_{n2} \quad [29]$$

The rolling force per unit width can be derived as:

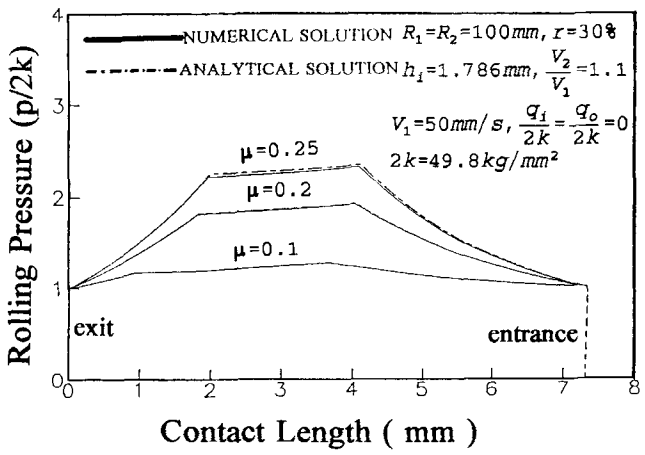

Fig. 3 Specific rolling pressure comparison of results obtained using the analytical method and the numerical method in asymmetrical rolling.

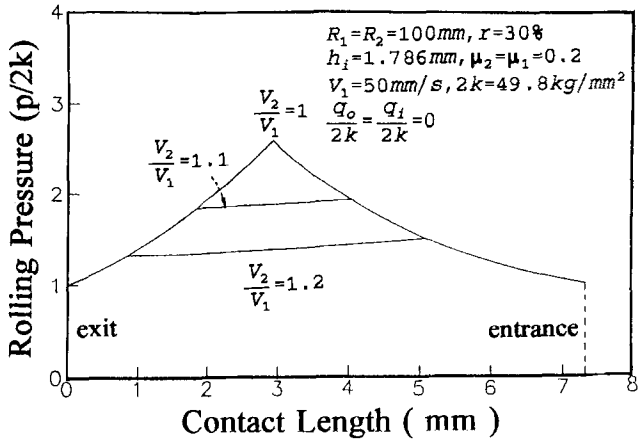

Fig. 4 Specific rolling pressure for various roll speed ratios.

$$P_{II} = 2k\int_{x_{n2}}^{x_{n1}} f_{II}dx = 2k[II_n + c_2(x_{n1} - x_{n2})] \quad [30]$$

where

$$II_n = x_{n1}\ln h_{n1} - 2x_{n1} + 2\sqrt{R_{eq}h_o}\tan^{-1}\frac{x_{n1}}{\sqrt{R_{eq}h_o}}$$

$$- x_{n2}\ln h_{n2} + 2x_{n2} - 2\sqrt{R_{eq}h_o}\tan^{-1}\frac{x_{n2}}{\sqrt{R_{eq}h_o}}$$

$$h_{n2} = h_o + \frac{x_{n2}^2}{R_{eq}},\ h_{n1} = h_o + \frac{x_{n1}^2}{R_{eq}}$$

It should be noted that Eq 28 to 30 are only valid for the case of $\mu_1 = \mu_2$.

2.6 *Limiting Analysis*

For the purpose of finding the limiting conditions, at which the rolling process cannot be achieved, for roll speed ratio and reduction, let x_{n2} be zero and $V_2 > V_1$, then Eq 19 becomes:

$$x_{n1} = R_1\sqrt{(V_A - 1)\frac{h_o}{R_A}} \quad [31]$$

Substituting the above equation into Eq 28, the following relationship can be derived:

$$c_1 e^{-a_1\omega_{n1}} - c_3 + \frac{2}{a_1}\left[\frac{\omega_{n1}^3}{3} - \frac{\omega_{n1}^2}{a_1} + s_1\omega_{n1}\right] - F = 0 \quad [32]$$

Note that the equation is valid only for $\mu_1 = \mu_2$. By this equation, the limiting condition between the roll speed ratio and reduction can be determined. Likewise, if $\mu_1 \neq \mu_2$, Eq 18 becomes:

$$c_1 e^{B_6\omega_{n1}} + \frac{2e^{a_2\omega_{n1}}}{a_1}\left[\frac{\omega_{n1}^3}{3} - \frac{\omega_{n1}^2}{a_1} + s_1\omega_{n1} - t_1\right]$$

$$- \frac{2e^{a_2\omega_{n1}}}{a_2}\left(\frac{\omega_{n1}^3}{3} - \frac{\omega_{n1}^2}{a_2} + s_3\omega_{n1} - t_2\right) - c_3 + B_5 = 0 \quad [33]$$

In Eq 32 and 33, ω_{n1} is the specific upper neutral position known, whereas V_A is the roll speed ratio to be determined. Consequently, V_A can be determined using the bisection numerical method.

For the case of front tension (q_o), the front tension cannot be increased so greatly that the neutral point x_{n1} is out of the contact arc, i.e., $x_{n1} > L$. The limiting (or critical) value of q_o, in which x_{n1} is equal to L, can be expressed as:

$$q_o = 2kf_o = 2k\left(c_3 - \frac{2t_3}{a_3}\right) \quad [34]$$

where

$$c_3 = e^{a_3\omega_{n2}}\left[c_1 e^{-a_1\omega_i} + \frac{2}{a_1}\left(\frac{\omega_i^3}{3} - \frac{\omega_i^2}{a_1} + s_1\omega_i\right)\right.$$

$$\left. - \frac{2}{a_3}\left(\frac{\omega_{n2}^3}{3} - \frac{\omega_{n2}^2}{a_3} + s_3\omega_{n2}\right) - F\right]$$

$$\omega_{n2} = \tan^{-1}\frac{x_{n2}}{\sqrt{R_{eq}h_o}}$$

$$x_{n2} = \sqrt{\frac{R_A L^2 - R_1^2(V_A - 1)h_o}{R_A V_A}}$$

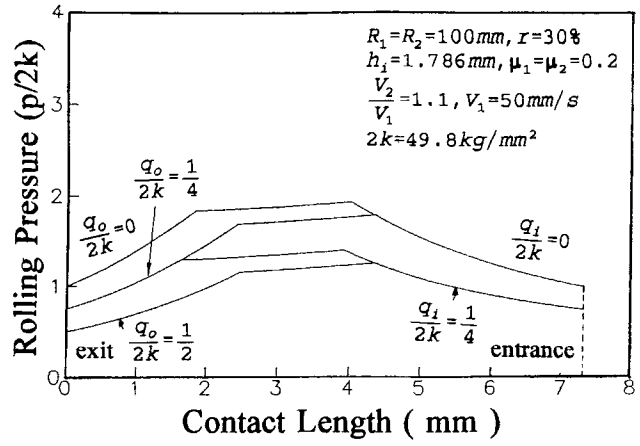

Fig. 5 Specific rolling pressure for various front and back tensions.

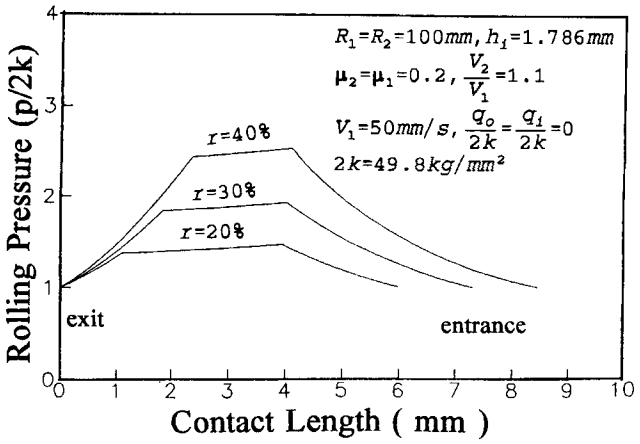

Fig. 6 Specific rolling pressure for various reductions.

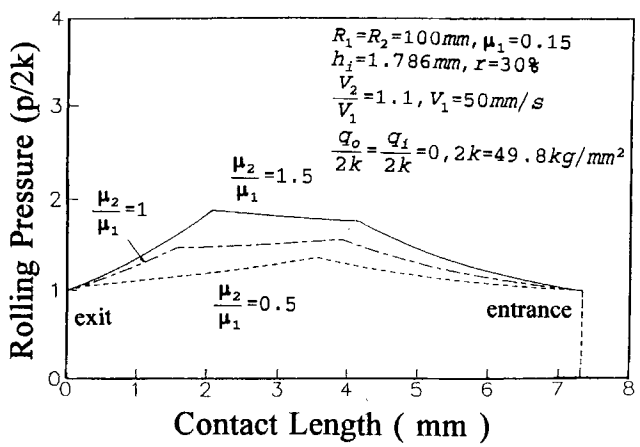

Fig. 7 Specific rolling pressure for various friction coefficient ratios.

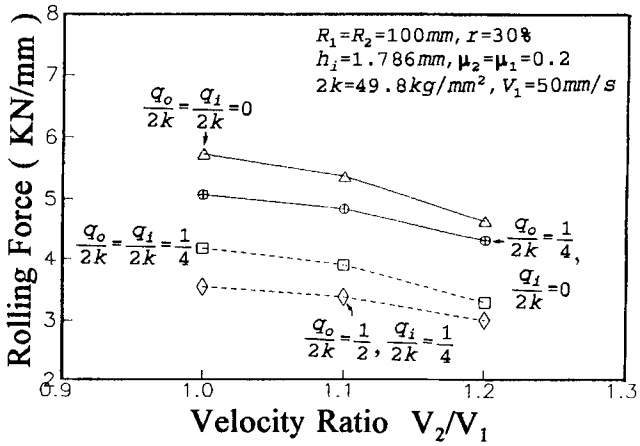

Fig. 8 Variation of rolling force with roll speed ratio for various front and back tensions.

3. Results and Discussion

To verify the accuracy of this analytical model, a comparison of the results obtained by the analytical method and those from the numerical method was performed, as shown in Fig. 3. The numerical results were obtained using the Runge Kutta method by simultaneously solving the governing equations, such as Eq 1, 2, and 4 for zone I, with the boundary conditions $p_o = 2k - q_o$ at $x = 0$ and $p_i = 2k - q_i$ at $x = L$, as well as the prediction equation for neutral points (Eq 19). When μ is small, both rolling pressure distributions coincide with each other. If μ is larger than 0.25, only a small margin of error exists. Hence, this newly proposed analytical model simulates the asymmetrical rolling process, with the added advantage of reduced calculation time. Generally, when the frictional coefficient increases, the rolling pressure increases, and the neutral points are positioned away from the exit.

Figure 4 shows that the rolling pressure decreases with increasing roll speed ratio, V_2/V_1, because the friction hill is cut off. Namely, the cross shear region (zone II), which causes the decrease in rolling pressure, widens with increasing roll speed ratio, V_2/V_1.

Figure 5 illustrates the rolling pressure distributions along the contact length with different back and front tensions. When front and back tensions are applied, the overall rolling pressure is reduced. Additionally, an increase in back tension causes the neutral points to move toward the exit, whereas an increase in front tension causes the neutral points to move toward the entry. The phenomenon is the same as in symmetrical strip rolling.

The variation in rolling pressure for different thickness reductions is illustrated in Fig. 6. It appears that the larger the reduction, the larger the rolling pressure, and the cross shear region (CSR) becomes narrower. Additionally, the position of the CSR moves toward the center of the contact length when the reduction increases.

Figure 7 shows the variation in rolling pressure with various frictional coefficient ratios, μ_2/μ_1. Obviously, the total rolling pressure increases with an increase in μ_2/μ_1, and the position of the neutral points moves toward the entrance of the roll-bite as

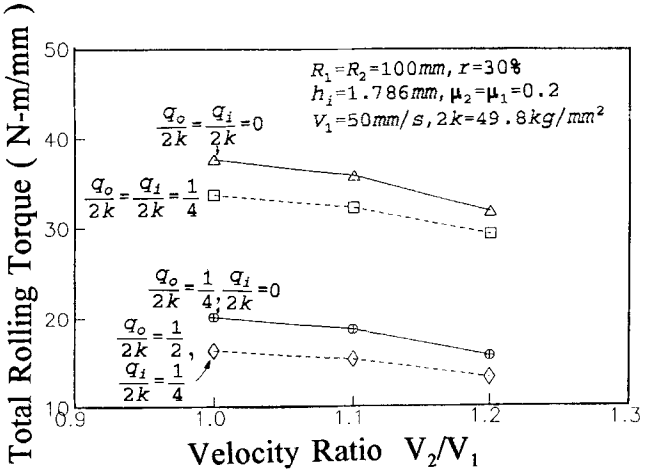

Fig. 9 Variation of rolling torque with roll speed ratio for various front and back tensions.

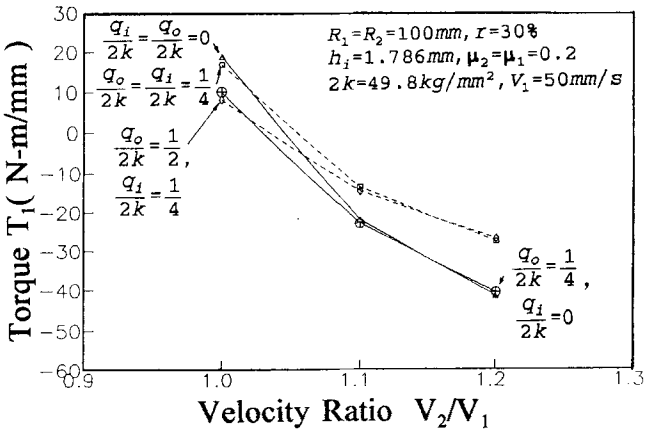

Fig. 10(a) Variation of low-speed rolling torque with roll speed ratio for various front and back tensions.

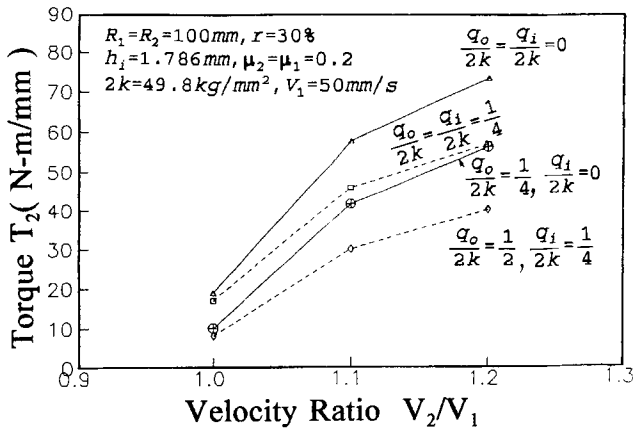

Fig. 10(b) Variation of high-speed rolling torque with roll speed ratio for various front and back tensions.

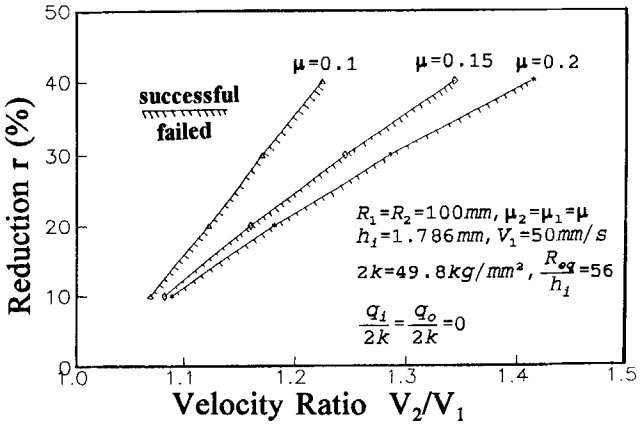

Fig. 11 Limiting diagram of reduction and roll speed ratio for various friction coefficients (such as $x_{n2} = 0$).

μ_2/μ_1 increases. However, the position of the neutral point of the upper roll moves faster than that of the lower roll. Consequently, the rolling pressure at the neutral point of the lower roll is larger than that at the neutral point of the upper roll as $\mu_2/\mu_1 = 0.5$, although the rolling pressure at the neutral point of the lower roll is less than that at the neutral point of the upper roll when $\mu_2/\mu_1 = 1.5$.

The effects of roll speed ratio, V_2/V_1, on rolling force and rolling torque are shown in Fig. 8 and 9, respectively. Rolling force and rolling torque are calculated by Eq 21, 25, and 26. It indicates, evidently, that both rolling force and rolling torque decrease with increasing roll speed ratio, V_2/V_1. However, rolling force decreases with increasing front and back tension, whereas the total rolling torque decreases with the deviation of front and back tension.

Figure 10(a) and (b) show the effect of variation in roll speed ratio on upper and lower roll torque. The upper roll torque, T_1, decreases with increasing roll speed ratio, whereas the lower roll torque, T_2, increases with increasing roll speed ratio, V_2/V_1. The total rolling torque, however, decreases with increasing roll speed ratio, as shown in Fig. 9.

Figure 11 shows the limiting condition between reduction, r, and roll speed ratio, V_2/V_1. For example, when $r = 30\%$, these limiting roll speed ratios are $V_2/V_1 = 1.17, 1.24, 1.29$ for $\mu = 0.1$, $\mu = 0.15$, $\mu = 0.2$, respectively. In other words, when $V_2/V_1 = 1.17$ for $\mu = 0.1$, the limiting reduction r cannot be greater than 30%, or the rolling process fails. This type of analysis is important in asymmetrical strip rolling process.

Figure 12 shows the effect of R_{eq}/h_i on the limiting reduction r. The limiting roll speed ratio, V_2/V_1, increases with increasing R_{eq}/h_i, because the average rolling pressure increase with increasing R_{eq}/h_i. From Fig. 12, note, for example, that when $r = 30\%$ for $\mu = 0.2$, these limiting roll speed ratios are $V_2/V_1 = 1.278$ ($R_{eq}/h_i = 50$), 1.306 ($R_{eq}/h_i = 80$), and 1.318 ($R_{eq}/h_i = 100$), respectively.

Figure 13 illustrates the effect of limiting roll speed ratio, V_2/V_1, on limiting reduction, r, and critical front tension, q_o. As $x_{n2} = 0$, which means that the neutral point x_{n2} reaches the exit of the roll gap earlier than x_{n1} reaches the entrance, it appears

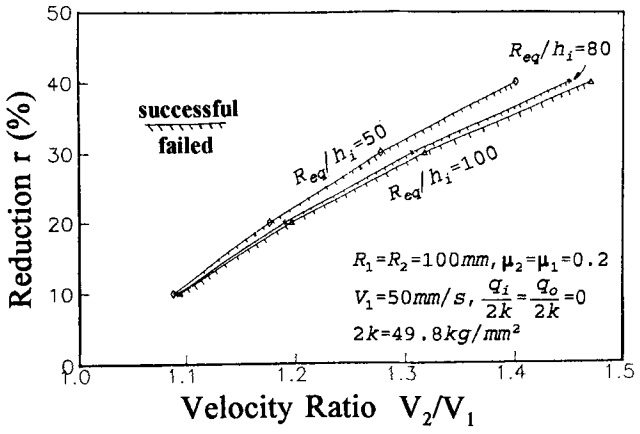

Fig. 12 Limiting diagram of reduction and roll speed ratio for various R_{eq}/h_i (such as $x_{n2} = 0$).

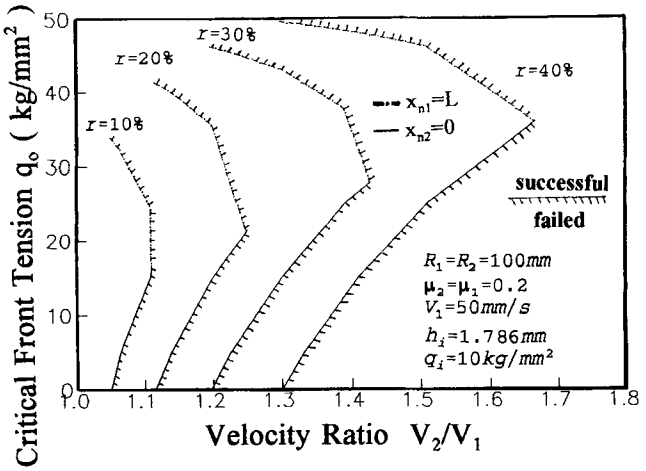

Fig. 13 Limiting diagram of front tension and roll speed ratio for various reductions (such as $x_{n1} = L$ or $x_{n2} = 0$).

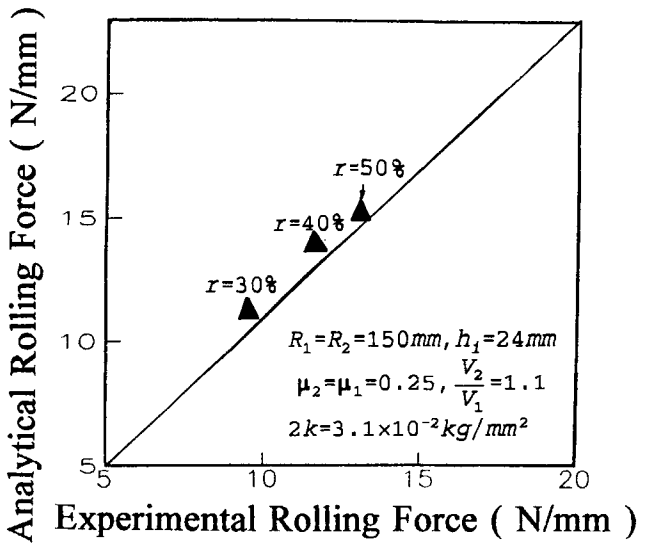

Fig. 14 Comparison of rolling force results obtained using the analytical method and experimental measurements.

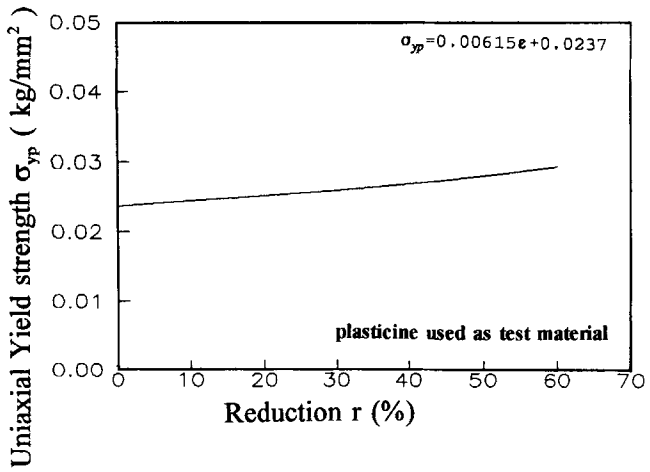

Fig. 15 Stress-strain curve.

that the critical front tension, q_o, increases, at the same reduction, r, with an increase in the limiting roll speed ratio, V_2/V_1. For $x_{n2} = 0$ and $r = 30\%$, these limiting roll speed ratios are $V_2/V_1 = 1.197$ ($q_o = 0$), 1.225 ($q_o = 5$ kg/mm^2), 1.3 ($q_o = 15$ kg/mm^2), 1.39 ($q_o = 25$ kg/mm^2), and 1.4278 ($q_o = 27.9$ kg/mm^2), respectively. As $x_{n1} = L$, which implies that the neutral point x_{n1} reaches the entrance of the roll gap earlier than x_{n2} reaches the exit, the limiting roll speed ratio increases, at the same reduction, with decreasing critical front tension, q_o. For $x_{n1} = L$, which denotes at the exit, when $r = 30\%$, the critical front tension, q_o, and roll speed ratio, V_2/V_1, are 46.247 kg/mm^2 (1.197), 45.541 kg/mm^2 (1.225), 43.12 kg/mm^2 (1.3), 37.674 kg/mm^2 (1.39), and 27.9 kg/mm^2 (1.4278), respectively. Figure 13 also illustrates that when reduction r increases in the same critical front tension q_o, the limiting roll speed ratio, V_2/V_1, increases because the average rolling pressure and the contact length are greater with increased reduction so as to bring about a larger limiting roll speed ratio, V_2/V_1.

For the purpose of proving the validity of this approach, a comparison of predicted rolling force with experimental measurements by Yamamoto[11] is shown in Fig. 14. The experiment was carried out using a two-high mill with plaster rolls, and the stress-strain curve of the plasticine used as the test material is shown in Fig. 15. The margin of error between the results of the rolling force obtained using this analytical method and the experimental measurement is only about 10%, which provides good consistency.

4. Conclusions

According to a series of analytical results, it is concluded that evaluation of rolling force and rolling torque by the present model is fast and accurate.

The rolling pressures obtained using this analytical model and a numerical method were compared. They agree with each other very well. Moreover, compared with experimental results, rolling force was predicted very accurately. Rolling pressure and rolling force can be significantly reduced using the asymmetrical rolling processes. Limiting rolling conditions, including reduction, roll speed ratio, and front tension, can be obtained easily, and rolling can be carried out successfully.

Using this model, one can quickly determine rolling pressure distributions, rolling forces, and rolling torques and limiting rolling conditions. It was concluded that the developed approach is acceptable and is able to offer systematic knowledge that is useful in designing asymmetrical cold strip rolling process.

Acknowledgments

This work is sponsored by the National Science Council of the Republic of China under grant No. NSC 81-0401-E-110-521. The advice and financial support of the National Science Council are gratefully acknowledged.

References

1. D. Rusia, Improvements to Alexander's Computer Model for Force and Torque Calculations in Strip Rolling Process, *J. Mater. Shap. Technol.*, Vol 8, 1990, p 167-177
2. D. Rusia, Review and Evaluation of Different Methods for Force and Torque Calculation in the Strip Rolling Process, *J. Mater. Shap. Technol.*, Vol 9, 1991, p 117-125
3. J.G. Lenard, Measurements of Friction in Cold Flat Rolling, *J. Mater. Shap. Technol.*, Vol 9, 1991, p 171-180
4. E. Orowan, The Calculation of Roll Pressure in Hot and Cold Flat Rolling, *Proc. Inst. Mech. Eng.*, Vol 150, 1943, p 140
5. H. Yamamoto et al., Effects of Peripheral Roll Speed and Friction Coefficients on Asymmetric Rolling Characteristics, *J. Jpn. Soc. Technol. Plasticity*, Vol 25 (No. 276), 1984, p 987-993
6. H. Shiozaki et al., "Effects of Roll Speed on the Rolling Force, Rolling Torque and Forward Slip in Cold Strip Rolling," Proc. Jpn. Soc. Technol. Plasticity, Spring Conf., 1979, p 391, in Japanese
7. H. Shiozaki et al., "Experimental Results due to Roll Speed in Asymmetric Rolling," Proc. Jpn. Soc. Technol. Plasticity, Spring Conf., 1978, p 33, in Japanese
8. H. Shiozaki et al., Experimental Study on the Effects of Differential Roll Speed Ratios on the Rolling Force, Rolling Torque and Forward Slip in Thin Strip Rolling, *J. Jpn. Soc. Technol. Plasticity*, Vol 23 (No. 262), 1982, p 1080
9. H. Yamamoto et al., "The Study on Asymmetrical Rolling (The Friction Model Analysis)," Proc. 33rd Joint Conf. Jpn. Soc. Technol. Plasticity, 1982, p 5, in Japanese
10. H. Yamamoto et al., "The Variation of Bending at Entrance with Friction Coefficient in Asymmetric Rolling," Proc. Jpn. Soc. Technol. Plasticity, Spring Conf., 1981, p 83, in Japanese
11. H. Yamamoto et al., "The Study on Asymmetric Strip Rolling (Plasticine Strain Analysis)," Proc. Jpn. Soc. Technol. Plasticity, Spring Conf., 1982, p 65, in Japanese
12. K. Nakajima et al., "Effects of Friction Coefficient on Asymmetric Strip Rolling," Proc. 31st Joint Conf. Jpn. Soc. Technol. Plasticity, 1980, p 451, in Japanese
13. H. Yamamoto et al., "The Study on the Minimum Rolled Strip Thickness in Asymmetric Strip Rolling," Proc. 32nd Joint Conf. Jpn. Soc. Technol. Plasticity, 1981, p 153, in Japanese
14. T. Kawanami et al., "The Asymmetric Rolling Analysis by FEM," Proc. Jpn. Soc. Technol. Plasticity, Spring Conf., 1986, p 235, in Japanese
15. M. Nakamura et al., "The Simplified Model Analysis in Cold Strip Rolling," Proc. Jpn. Soc. Technol. Plasticity, Spring Conf., 1983, p 451, in Japanese